Vegetable Research

ARTICLE

Open Access

https://doi.org/10.48130/VR-2022-0017
Vegetable Research **2022**, 2:17

BrDDB1A maintains regular growth of Chinese cabbage via UV tolerance

Meidi Zhang[1,2#], Jiaqi Zou[1#], Shengnan Huang[1], Wei Fu[1], Yue Gao[1], Gaoyang Qu[1], Yonghui Zhao[1], Ying Zhao[1], Zhiyong Liu[1], and Hui Feng[1*]

[1] *College of Horticulture, Shenyang Agricultural University, 120 Dongling Road, Shenhe District, Shenyang 110866, China*
[2] *College of Agriculture, Jilin Agriculture Science and Technology University, 77 Hanlin Road, Changyi District, Jilin 132101, China*
[#] These authors contributed equally: Meidi Zhang, Jiaqi Zou
[*] Corresponding author, E-mail: fenghuiaaa@syau.edu.cn

Abstract

Normal plant growth and development ensures the timely maturity and expected yield of crops. The repair mechanism of genome damage under adverse circumstances is essential for maintaining regular plant growth. Herein, two allelic growth retardation mutants of Chinese cabbage, *grm1* and *grm2*, were obtained from EMS-mutagenized populations of wild-type 'FT' isolated-cultured microspores and seeds, respectively. Both mutants stably inherited and exhibited stunted growth with smaller leafy-heads. Genetic analysis and allelism test manifested that the mutated trait was triggered by a same single recessive nuclear gene. Via BSR-Seq, *Brgrm1* was mapped to a target region including 20 genes on chromosome A09. Whole-genome re-sequencing revealed that *BraA09g024830.3C* in *grm1* had a single base (A) deletion in the 17th exon, leading to a termination codon (TAG). Genotyping showed that the mutated phenotype co-segregated with the InDel in recombinants of the closest linkage markers. In addition, cloning of *BraA09g024830.3C* in *grm2* found that a base substitution (G-A) occurred in the last base of the 1st intron causing an additional 263-bp retention in coding sequences, which in turn led to a termination codon (TAA). *BraA09g024830.3C* (*BrDDB1A*) is a homolog of *Arabidopsis thaliana Damaged DNA Binding Protein 1A* (*DDB1A*), a key gene of UV tolerance involved in DNA damage repair. The two mutants exhibited normal plant growth identical with wild-type under an extremely low UV radiation. Our results demonstrated that *BrDDB1A* contributes to maintaining regular plant growth in Chinese cabbage, which provide insights into elucidating the molecular mechanism underlying Chinese cabbage growth and development.

Citation: Zhang M, Zou J, Huang S, Fu W, Gao Y, et al. 2022. *BrDDB1A* maintains regular growth of Chinese cabbage via UV tolerance. *Vegetable Research* 2:17 https://doi.org/10.48130/VR-2022-0017

INTRODUCTION

The normal growth of plants is the premise of survival and propagation, enabling crops to mature in time and obtain the expected yield. Light serves as the source of energy and developmental switch throughout the plant life cycle, thereby dramatically determining plant growth and architecture[1]. Plants alter their morphological and growth features responding to light signals of varying intensity and quality for their survival and optimal growth[1,2]. Ultraviolet (UV) radiation occupies a minor fraction of sunlight, yet it imparts many positive and negative effects on plant growth[2]. The increasingly enhanced UV radiation in solar radiation due to global warming would potentially induce DNA damage[3]. DNA damage affects cellular functionality and disturbs the normal growth of the whole organism[4]. Plants are constantly exposed to endogenous cellular processes and exogenous environmental events, which can impair genomic integrity through DNA damage[5]. Effective DNA damage detection mechanisms that enable the cells to quickly activate repair mechanisms are crucial for maintaining genomic integrity[6].

All organisms possess the mechanisms for repairing DNA damage[7]. Because of the sessile lifestyle, plants have developed many ways to protect themselves from UV radiation in sunlight. For example, some UV absorbing pigments are synthesized in plant leaves; various DNA repair mechanisms are expressed to repair UV induced damage. The repair of UV-damaged DNA is mainly performed by two pathways, light-dependent repair and light-independent (dark) repair[8]. Light-dependent repair utilises photoreactivation, which is primarily a form of repair for lower organisms and as organisms evolve. Light-independent repair is known as nucleotide excision repair (NER)[9], which does not directly reverse the DNA damage but replaces DNA damage with undamaged nucleotides[10,11]. In *Arabidopsis*, *RAD23*, *DDB1A*, *CSA*, and *XPB* are involved in this pathway, and *DDB1A* is recognized as a key gene essential for the DNA repair process[12–15].

Damage DNA Binding Protein 1A (DDB1A) is involved in the damage recognition stage of the NER pathway. DDB1 was first identified in patients with human xeroderma pigmentosum who are hypersensitive to UV-B radiation because of defects in DNA repair[16–18]. Subsequently, the homologous gene of *DDB1* was found in plants such as *Arabidopsis*, tomato, and rice. *Arabidopsis* has two highly related DDB1 proteins, named DDB1A and DDB1B. A null mutant (*ddb1a*) of *DDB1A* was constructed in *Arabidopsis* and this mutant showed some different phenotypes from the wild-type plants; for example, the *ddb1a* mutant had significantly longer hypocotyls, more lateral roots, and fewer rosette leaves and the shoot height was

significantly reduced compared to that in the wild-type[13]. Bernhardt et al.[13] revealed that DDB1A is critical for embryo development and affects whole plant development. Two *high-pigment-1* (*hp-1*) and *high-pigment-1^w* (*hp-1^w*) mutants were obtained in tomato with the phenotype displaying higher anthocyanin levels, shorter hypocotyls, and enhanced fruit pigmentation compared to their semi-isogenic wild-type counterparts[19]. Lieberman et al.[20] found that the higher anthocyanin level phenotypes in *hp-1* and *hp-1^w* were controlled by the same gene, *DDB1*. Ishibashi et al.[21] cloned *DDB1* in rice, with resulting characterization indicating that *DDB1* is mainly expressed in proliferative tissue, with increased expression after UV radiation. These results indicated that *DDB1* expression is related to cell proliferation and might primarily be required for DNA repair during DNA replication. Further, *DDB1A* performs not exactly the same function in different species.

Plant mutants exhibiting growth retardation-related phenotypes such as diminished growth and sensitive responses to UV radiation are conductive to characterize the function of genes linking growth to light-dependent DNA repair[2,22–25]. In this study, we screened two allelic mutants with retarded growth, *grm1* and *grm2*, from EMS-mutagenized populations of Chinese cabbage wild-type 'FT'. These mutants exhibited stunted vegetative growth with smaller leafy-heads, and their mutated trait stably inherited. Their causal gene was mapped to the *BraA09g024830.3C* (*BrDDB1A*) on A09 chromosome, which encodes the putative Damaged DNA Binding Protein 1A in Chinese cabbage. The mutants exhibited normal growth and morphology identical with the wild-type in a low UV-radiation environment. Our results demonstrated that BrDDB1A is required for maintaining regular plant growth, which provide evidence for characterizing the functional gene in DNA repair associated with Chinese cabbage growth.

MATERIALS AND METHODS

Plant material and phenotypic identification

The *grm1* mutant was obtained by constructing a mutant library as previously described by Huang et al.[26]. Isolated 'FT' microspores from the Chinese cabbage doubled haploid (DH) line were treated with 0.16% EMS for 15 min[27]. *grm2* with the same phenotype as *grm1* was selected from the mutant library constructed with 0.8% EMS-treated germinated 'FT' Chinese cabbage seeds. The stable inheritance of *grm1* and *grm2* mutants was exhibited after multiple generations.

When the third true leaf appeared in *grm1* and *grm2* mu tants, the leaf length, leaf width, and plant width of five plants were measured every 3 d for a total of 22 d. The fresh weight and dry weight of three plants were measured every 6 d for 45 d. At the heading stage, the head length, head width, and head weight of five plants were measured.

UV sensitivity assays

To investigate whether the growth of two *grm* mutants would be sensitive to UV, we simultaneously sowed 100 *grm1*, 100 *grm2* and 100 wild-type 'FT' under the same environmental conditions, and randomly selected 50 plants of each at the seedling stage (3rd leaf stage, 18 d after seeding) as the control and the experimental group, respectively. The control group (50 *grm1*, 50 *grm2* and 50 wild-type 'FT') was grown in the greenhouse under natural conditions (day length of 16 h/8 h, 22–25 °C/15–18 °C day/night regime). The experimental group (50 *grm1*, 50 *grm2* and 50 wild-type 'FT') was grown in an artificial climate chamber for plant growth, in which photoperiod and ambient temperature were in accordance with those of the control group. The growth of the two plant groups was observed from the seedling stage (18 d after seeding) to the rosette stage (40 d after seeding). The average maximum UV intensity perpendicular to the plants surfaces under the two conditions was 1.89 mW/m^2 and 0.01 mW/m^2, as measured with a UV meter (Tenmars-TM213).

Scanning electron microscopy (SEM) observation

The third true leaf of *grm1* and *grm2* mutants were observed by SEM (Hitachi, Japan) as previously described[28].

Genetic analysis

To investigate the genetic inheritance of *grm1* and *grm2* mutants, F_1, F_2, and BC_1 generations were constructed by crossing 'FT' plants with *grm1* and *grm2* mutants. The segregation ratio of F_2 and BC_1 generations was analyzed using the Chi-squared (χ^2, $\chi^2_{0.05,1} = 3.84$) test. To determine whether the target gene of the two mutants (*grm1* and *grm2*) was allelic, a cross between *grm1* and *grm2* mutants was performed.

Mapping population construction and BSR-Seq analysis of *grm1*

The *grm1* mutant was crossed with '15A110', a DH line of Chinese cabbage. In the F_2 mapping population (*grm1* crossed with '15A110'), two extreme mixed pools, a mutant pool (LM-pool), and a normal pool (WT-pool) were constructed for BSR-Seq. The total RNA was extracted using an RNApure Total RNA Kit (Aidlab, Beijing, China). Pass filter data were obtained on an Illumina HiSeq 2500 platform by GENEWIZ (Suzhou, China). Clean reads were obtained using Cutadapt software (version 1.9.1) to filter low quality data and remove contamination and joint sequences. Clean reads were compared with the reference genome for analysis by Hisat software (v2.0.14)[29]. By comparing the results of each sample with the reference genome, mpileup processing was carried out using SAMtools (v0.1.18) software to obtain the possible single-nucleotide variant (SNV) results of each sample. SNV results were annotated using ANNOVAR (v2013.02.11) software. Euclidean distance (ED) was used to estimate the genetic distance between SNVs and the target trait. ED was calculated as follows:

$$ED = \sqrt{(\mathrm{AF}-\mathrm{AS})2+(\mathrm{CF}-\mathrm{CS})2+(\mathrm{GF}-\mathrm{GS})2+(\mathrm{TF}-\mathrm{TS})2}$$

A, C, G, and T represented the corresponding bases in the F-pool and S-pool. For example, AF indicates the frequency of the 'A' base in the F-pool[30]. To eliminate background noise, the ED value of each different SNV site was processed to the power of 5 (ED^5)[31]. All ED^5 values were sorted and the SNV sites corresponding to the top 1% of ED^5 values were screened. Specific chromosome regions were further located according to the distribution of differential SNV sites.

DNA extraction and linkage analysis

The cetyltrimethyl ammonium bromide (CTAB) method was used to extract the DNA of two parents (*grm1* and '15A110') and 3,022 F_2 recessive homozygous plants, according to the method of Murray & Thompson[32] with minor modifications. According to the BSR-Seq result, the simple sequence repeats (SSRs) and insertion/deletion (InDel) markers were designed by Primer Premier5 software and synthesized in GENEWIZ (Suzhou, China). The polymorphic markers were screened for linkage analysis. PCR was used to amplify the DNA, and

polyacrylamide gel electrophoresis was used to examine the PCR products as previously described by Huang et al.[26].

Whole-genome re-sequencing

For whole-genome re-sequencing, *grm1* mutant and 'FT' DNA was extracted using a DNA Secure Plant Kit (Tiangen, Beijing). Two libraries with inserted fragments of 400 bp were constructed and paired-end sequencing was performed on the *grm1* mutant and 'FT' libraries using an IlluminaHiSeq sequencing platform and next-generation sequencing technology. Clean reads were obtained by filtering raw reads according to the following requirements: (1) removal of joint contamination using Adapter Removal (version 2)[33]; (2) the sliding window method was used to filter the low-quality reads; (3) removal of reads ≤ 50 bp. BWA (0.7.12-r1039) [34] software was used to compare the clean reads to the reference genome (Brassica_rapaV3.0) using the mem program according to default parameters. GATK software[35] was used for single nucleotide polymorphism (SNP) and InDel detection. ANNOVAR[36] software was used to annotate SNP and InDel loci.

Candidate gene analysis

According to the gene sequence information, primers were designed to amplify full-length coding sequences (CDs) and promoter sequences of candidate genes from *grm1*, *grm2,* and 'FT' samples. The amplified products were purified using a Gel Extraction Kit (Omega, USA), and then, the purified products were ligated into the pGEM -T Easy Vector (Promega, USA) and finally transformed into TOP10 competent cells (CWBIO, China). The recombinant plasmids were sequenced in GENEWIZ (Suzhou, China). The sequence analysis was performed using DNAMAN software (v6.0.3.99).

RT-qPCR analysis

Brgrm1 expression was compared between *grm1* and 'FT' samples. Different organs (root, stem, leaf, flower, bud, pod) and leaves from different periods (the cotyledon, the first true leaf, the third true leaf, the sixth true leaf, the rosette leaf, the head leaf) served as templates for RT-qPCR. Total RNA was extracted using an RNApure Total RNA Kit (Aidlab, Beijing, China) and reverse-transcribed into cDNA using FastQuant RT Super Mix (Tiangen, China). cDNA was used as a template with primers for RT-qPCR analysis. Primer sequences are shown in Supplemental Table S1. RT-qPCR products treated with 2× UltraSYBR mixture (Low Rox) (CWBIO, China) were evaluated using the QuantStudio 6 Flex Real-Time PCR System (Applied Biosystems, USA). Three biological replicates were used for each test. Expression levels were calculated using the $2^{-\Delta\Delta CT}$ method[37] with *Actin* serving as an internal control.

Bioinformatics analysis

The SMART software (http://smart.embl-heidelberg.de/) was used to predict the conserved domains of the candidate gene. The tertiary structure of the protein encoded by the candidate gene was predicted using Phyre2 software (www.sbg.bio.ic.ac.uk/phyre2/html/page.cgi?id=index). Subcellular localization of the protein was predicted via Plant-mPLoc (www.csbio.sjtu.edu.cn/bioinf/plant-multi/#). The predicted nucleus localization of BrDDB1A was analyzed using INSP[38] (Identification Nucleus Signal Peptide) prediction software at: www.csbio.sjtu.edu.cn/bioinf/INSP/.

Statistical analysis

The error values were calculated to measure the accuracy of the data; to reduce error values, three biological replicates were used. Significant differences were assessed using the IBM SPSS Statistics software (v22.0.0.0).

RESULTS

Morphological characterization of *grm1* and *grm2*

grm1 and *grm2* mutants both displayed growth retardation with a smaller leafy head compared to the 'FT' phenotype (Fig. 1 and Table 1). The growth curve showed that the growth rate of *grm1* and *grm2* mutants was slower than 'FT' growth; the difference in leaf length, leaf width, and plant width was significant at 9–15 d (Supplemental Fig. S1a–c). The fresh and dry weights of *grm1* and *grm2* mutants were dramatically lower than those of 'FT' plants (Supplemental Fig. S1d, S1e). SEM results showed that the number of cells in *grm1* and *grm2* mutants was higher than those in 'FT' plants at the same location and period. Correspondingly, cell size in *grm1* and *grm2* mutants was smaller than that in 'FT' plants (Fig. 2).

Allelism of *grm1* and *grm2*

The *grm1* and *grm2* were identified from EMS-mutagenized populations of wild-type 'FT' isolated-cultured microspores and seeds, respectively, but they both exhibited very similar growth retardation phenotype. Therefore, to confirm whether their mutant phenotype might be caused by the same gene, we conducted cross pollination between *grm1* and *grm2* for testing their allelism. It was found that the phenotype of all 50 plants in the hybrid F_1 generation from *grm1* plants crossed with *grm2* plants was consistent with the mutant phenotype (Fig. 1e, f). This result indicated that *grm1* and *grm2* were caused by allelic mutation.

Inheritance of mutant trait in *grm1* and *grm2*

The genetic inheritance of the *grm1* and *grm2* mutants was calculated. The segregation ratio of *grm1* F_2 and BC_1 generations are listed in Table 2 and the segregation ratios of *grm2*, F_2, and BC_1 generations are listed in Table 3. For *grm1* mutants, all F_1 generation plants showed the 'FT' phenotype. Of a total of 553 F_2 individuals, 130 plants displayed the mutant phenotype, whereas 423 plants displayed the 'FT' phenotype; the F_2 segregation ratio was approximately 3:1. Of a total of 106 BC_1 plants, 45 and 61 plants displayed mutant and 'FT' phenotypes, respectively; the BC_1 segregation ratio was approximately 1:1. Overall, these results indicated that the *grm1* mutant trait was controlled by a single nuclear recessive gene (*Brgrm1*). The segregation ratios of *grm2* F_2 and BC_1 generations were also 3:1 and 1:1, respectively. The *grm2* mutant trait was thus also controlled by a single nuclear recessive gene (*Brgrm2*).

Primary mapping of *Brgrm1* to chromosome A09 by BSR-Seq

The *grm1* F_2 population was used to map the target region by BSR-Seq. Approximately 40,000,000 clean reads were obtained from the LM-pool and WT-pool. The ED^5 value of SNV differences was plotted in the reference genome. The distribution of ED^5 values on the chromosomes is shown in Fig. 3. *Brgrm1* was mapped to chromosome A09. Using the top 1% of ED^5 values as a threshold, five intervals were obtained on chromosome A09 (Supplemental Table S2). SSR markers were designed, two parents (*grm1* and '15A110') were used to screen the linkage marker, and 300 F_2 individuals were used to verify the target region (Supplemental Fig. S2). Finally, *Brgrm1* was

Fig. 1 Phenotypic characterization of the wild-type 'FT' and *grm1* and *grm2* mutants. (a) The wild-type 'FT' at seedling stage. (b) *grm1* at seedling stage. (c) *grm2* at seedling stage. (d) The phenotype of 'FT' (left), *grm1* (middle), and *grm2* (right) at rosette stage. (e) The phenotype of *grm2* (left), F1 (middle, *grm2* × *grm1*), and *grm1* (right) at rosette stage. (f) Leafy heads of the *grm1* (left) and wild-type 'FT' (right). (g) Leafy heads of the *grm2* (left) and wild-type 'FT' (right).

Table 1. Identification of agronomic characters in *grm1*, *grm2* and wild-type 'FT' at the heading stage

Characteristics	'FT'	*grm1*	*grm2*
Mean of head weight (kg)	0.41 ± 0.05	0.10 ± 0.00*	0.16 ± 0.03*
Mean of head length (cm)	12.73 ± 0.68	11.14 ± 0.11*	11.71 ± 0.32*
Mean of head width (cm)	9.22 ± 0.82	5.88 ± 0.07*	6.35 ± 0.29*
Mean of head length/head width ratio	1.38 ± 0.09	1.89 ± 0.01*	1.84 ± 0.05*

mapped between the SSR markers ZMD-9 and ZMD-44 on chromosome A09; the genetic distances were 1.52 cM and 1.79 cM, respectively (Fig. 4a).

Fine mapping of *Brgrm1*

To map *Brgrm1*, more SSR and InDel markers were designed between the ZMD-9 and ZMD-44 markers. Of these, six polymorphic markers, XD-5, XD-11, ZMD-63, XD-24, ZMD-65, and ZMD-21, were screened (Supplemental Table S1). A total of 3022 F_2 individuals were used to locate *Brgrm1*. The label of

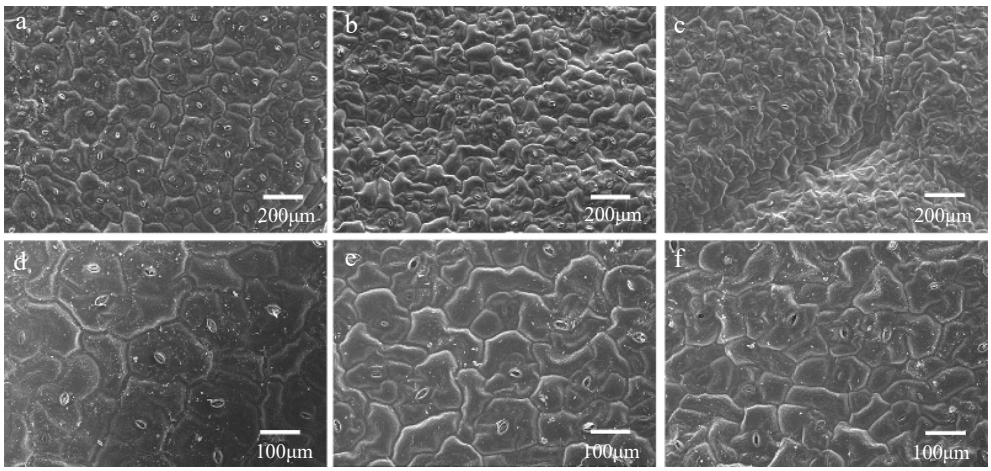

Fig. 2 Observation of the leaf epidermal cells by scanning electron microscopy (SEM). (a) 'FT' at 200 μm, (b) *grm1* at 200 μm, (c) *grm2* at 200 μm, (d) 'FT' at 100 μm, (e) *grm1* at 100 μm, (f) *grm2* at 100 μm.

Table 2. Genetic analysis of the *grm1* mutant.

Generation	Total	'FT'	*grm1*	Segregation ratio	χ^2
P_1 ('FT')	50	50	0		
P_2 (*grm1*)	50	0	50		
F_1 ($P_1 \times P_2$)	50	50	0		
F_1 ($P_2 \times P_1$)	50	50	0		
BC_1 ($F_1 \times$ 'FT')	90	90	0		
BC_1 ($F_1 \times$*grm1*)	106	61	45	1.356:1	2.424
F_2	553	423	130	3.254:1	0.699

Table 3. Genetic analysis of the *grm2* mutant.

Generation	Total	'FT'	*grm2*	Segregation ratio	χ^2
P_1 ('FT')	50	50	0		
P_2 (*grm2*)	50	01	50	1	
F_1 ($P_1 \times P_2$)	50	50	0		
F_1 ($P_2 \times P_1$)	50	50	0		
BC_1 ($F_1 \times$ 'FT')	100	100	0		
BC_1 ($F_1 \times$ *grm2*)	150	78	72	1.083:1	0.24
F_2	300	231	69	3.348:1	0.682

recombinants indicated that XD-5 and XD-11 were located on one side, and ZMD-63, XD-24, ZMD-65, and ZMD-21 were located on the other side of *Brgrm1*. Finally, *Brgrm1* was mapped between the XD-11 and ZMD-63 markers with a physical distance of 172.85 kb. Both XD-11 and ZMD-63 markers had one recombinant, and the genetic distance was 0.01 cM (Fig. 4b).

Identification of the mutant gene by whole-genome re-sequencing

Twenty genes were contained in the target region (Fig. 4c and Supplemental Table S3). Whole-genome re-sequencing was used to predict the candidate gene. In total, 67,518,344 and 93,975,642 clean reads were obtained from the *grm1* mutant and 'FT', respectively. Comparisons of the results between *grm1* and 'FT' provided 1,075,244 SNPs and 389,539 InDels from the *grm1* mutant and 1,363,821 SNPs and 368,451 InDels from 'FT' samples. The criteria for mutation screening were 1) the mutations occurred in the target region and 2) the mutations were homozygous and non-synonymous. The results suggested that one InDel was screened in the target region of the *grm1* mutant. A base deletion (A) occurred in the 17th exon of *BraA09g024830.3C*. Gene annotation indicated that *BraA09g024830.3C* encoded the Damaged DNA Binding Protein 1A, which plays a role in damaged DNA repair. Therefore, *BraA09g024830.3C* was regarded as the candidate gene.

Cloning and co-segregation analysis of the candidate gene

The primers (Supplemental Table S1) were designed to clone the full length (B-1~B-9) and CDs (CD-1~CD-5) of *BraA09g024830.3C* from *grm1* mutant and 'FT'. Cloning and sequencing results showed that the base (A) deletion in the 17th exon (Fig. 5a) caused a frameshift mutation, ultimately resulting in the termination of amino acid coding (Fig. 5b). Three primers (Pro-1~Pro-3) (Supplemental Table S1) were designed to clone the promoter sequence of *BraA09g024830.3C*

Fig. 3 ED^5 (Euclidean distance to the power of 5) distribution of filtered single nucleotide polymorphisms (SNPs) on chromosomes based on bulked segregant RNA-seq (BSR-Seq). Note: X-axis represents the chromosome in *Brassica rapa* and Y-axis represents the ED^5 values of filtered SNPs. The horizontal line is the correlation threshold of the top 1%.

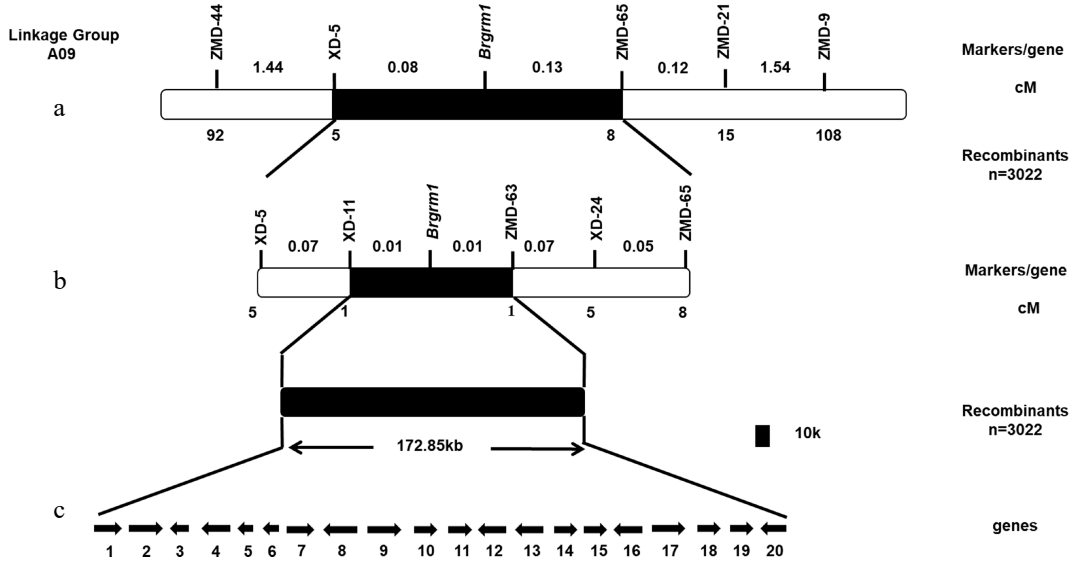

Fig. 4 Construction of genetic and physical maps of *Brgrm1* and analysis of candidate genes. (a) Preliminary mapping of *Brgrm1*. (b) Fine mapping of *Brgrm1*. (c) Candidate gene analysis in target region. Arrows indicate the direction of gene transcription.

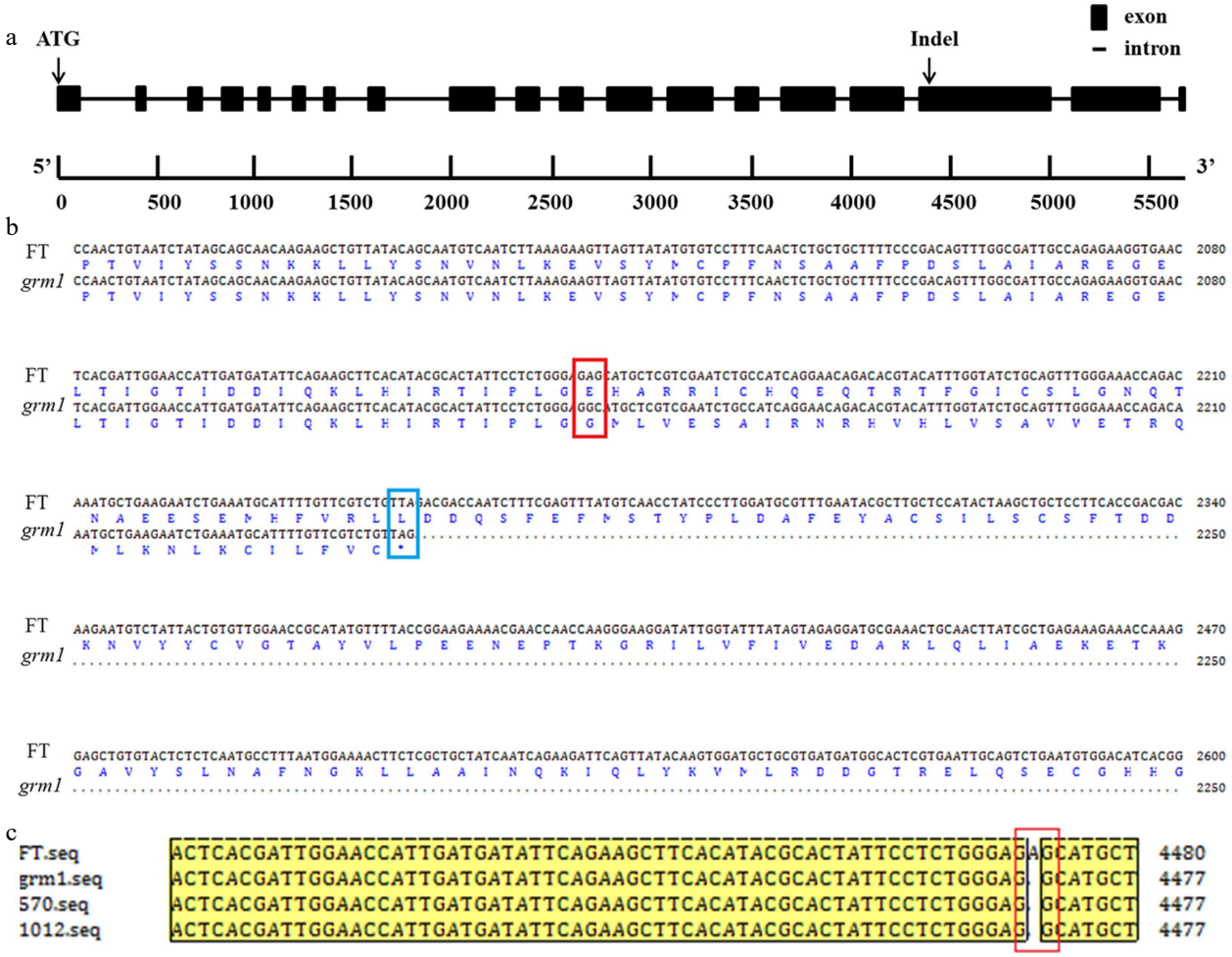

Fig. 5 Gene structure and amino acid sequence alignment. (a) Gene structure of *BraA09g024830.3C* with an insertion/deletion (InDel). (b) Alignment of nucleotide sequence and amino acid sequence of *BraA09g024830.3C* from 'FT' and *grm1* mutant. The site created by the non-synonymous single nucleotide polymorphism (SNP) is shown by a red empty box and the coding termination is shown by a blue empty box. (c) Alignment of *BraA09g024830.3C* with nucleotide sequences in the two F_2 recombinants, the *grm1* mutant, and 'FT'. Note: the two F_2 recombinants were from the most closely linked markers, XD-11 and ZMD-63.

from the *grm1* mutant and 'FT'. The result showed that the promoter sequence of *BraA09g024830.3C* was not different between *grm1* and 'FT'. To further validate the mutation locus, two recombinants of the two closest markers were cloned. The result showed that the two recombinants had the same base deletion compared to the sequence of the *grm1* mutant in the 17th exon (Fig. 5c). Therefore, this InDel was co-segregated with the growth retardation trait. These results showed that *BraA09g024830.3C* was the strongest candidate gene.

Cloning of *BraA09g024830.3C* in the *grm2* mutant

As *grm1* and *grm2* were triggered by the allelic mutations, the promoter sequence and full-length sequence and CDs of *BraA09g024830.3C* were also cloned from the *grm2* mutant. The result showed that the promoter sequence of *BraA09g024830.3C* was not different between *grm2* and 'FT'. The resulting full-length clone indicated that a base substitution (G to A) occurred in the first intron of *grm2* (Fig. 6a, b). The cloning and sequencing of CDs showed that the first intron with 263 bp was retained in *grm2* and resulted in a frameshift mutation, ultimately leading to a termination amino acid codon (TAA) (Fig. 6c). These results showed that *BraA09g024830.3C* was the causal gene, which accounts for the phenotype of growth retardation in Chinese cabbage, and it was named *BrDDB1A*.

Expression analysis of *BrDDB1A* in the *grm1* and *grm2* mutant

RT-qPCR detection of the *BrDDB1A* expression levels in *grm1*, *grm2*, and 'FT' showed that *BrDDB1A* expression from different organs (root, stem, leaf, flower, bud, pod) was dramatically lower in *grm1* than in 'FT' (Fig. 7a), and *BrDDB1A* expression in *grm1* and *grm2* leaves from different periods (the cotyledon, the first true leaf, the third true leaf, the sixth true leaf, the rosette leaf, the head leaf) was significantly lower than that in 'FT' (Fig. 7b, c).

Bioinformatics analysis of BrDDB1A

The SMART software showed that the conserved domain of BrDDB1A was different in the two mutants from that in 'FT' (Fig. 7d). BrDDB1A had two conserved domains, MMS1_N and CPSF_A in 'FT'; in contrast, it had only one conserved domain, MMS1_N, in *grm1* and had no conserved domains in *grm2*. Additionally, the Phyre2 results showed that the protein tertiary structure was changed in the two mutants compared with that in 'FT' (Fig. 7e). BrDDB1A in 'FT' contained three β-propeller (βPa–βPc) subdomains: an independent β-propeller (BP) domain (BPB) and a clam-shaped double-propeller fold (BPA-BPC). Conversely, in *grm1*, the base deletion led to the disappearance of the BPA domain from BrDDB1A and destroyed the structure of the clam-shaped double-propeller fold. Additionally, in *grm2*, the intron retention resulted in the disappearance of both the BPB and BPA-BPC domains. Importantly, different variations of the same gene in the two mutants led to changes in the BrDDB1A tertiary protein structure. Meanwhile, the subcellular localization of BrDDB1A was predicted via Plant-mPLoc, it was found that *BrDDB1A* might encode a nucleus-localized protein (Supplemental Fig. S3).

Mutation of BrDDB1A induced UV-sensitive growth

It has been reported that overexpression of *Arabidopsis* DDB1A enhances UV tolerance[11]. To investigate whether the dysfunction of the BrDDB1A in the two *grm* mutants makes them sensitive to UV, we observed two groups of 50 mutants and 50 wild-type plants that grew in different growth

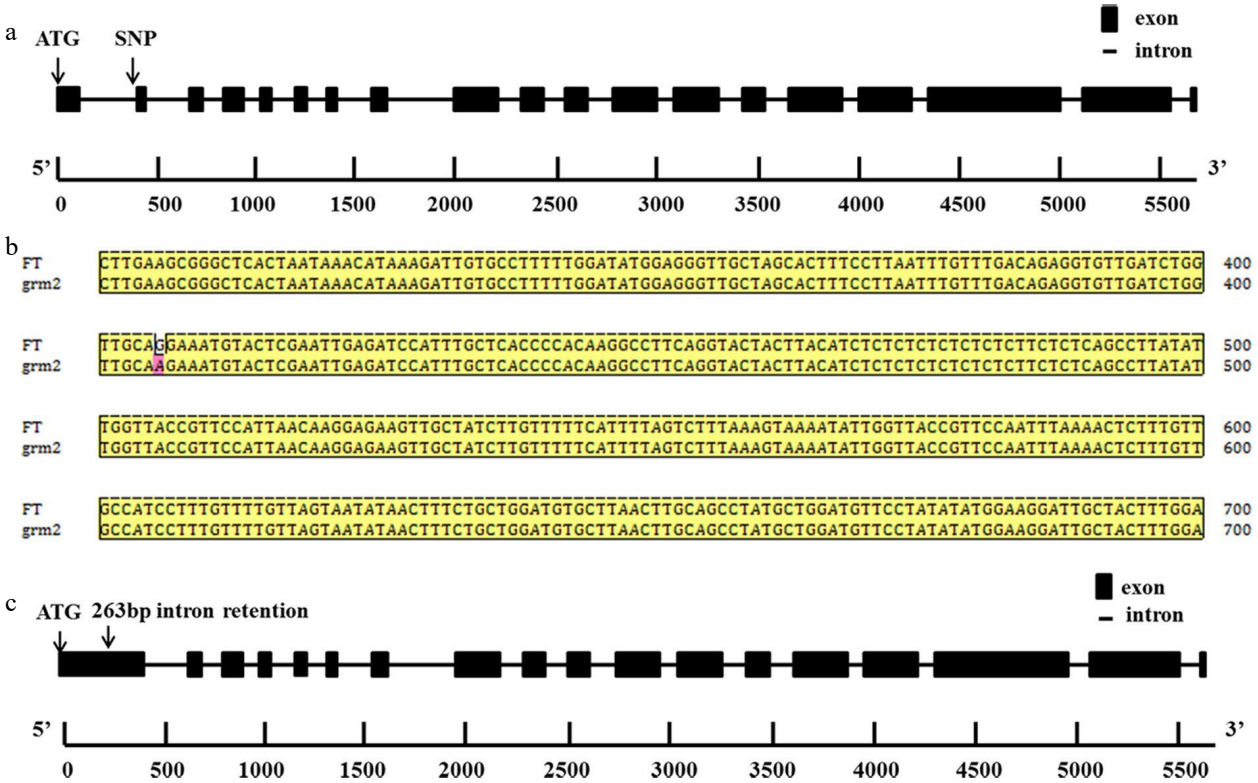

Fig. 6 Gene structure and nucleotide sequence alignment. (a) Gene structure of *BrDDB1A* in *grm2* with a single nucleotide polymorphism (SNP). (b) Nucleotide sequence alignment of *BrDDB1A.3C* in 'FT' and *grm2* mutant. c 263-bp intron retention occurred in the first intron of *BrDDB1A* in the *grm2* mutant.

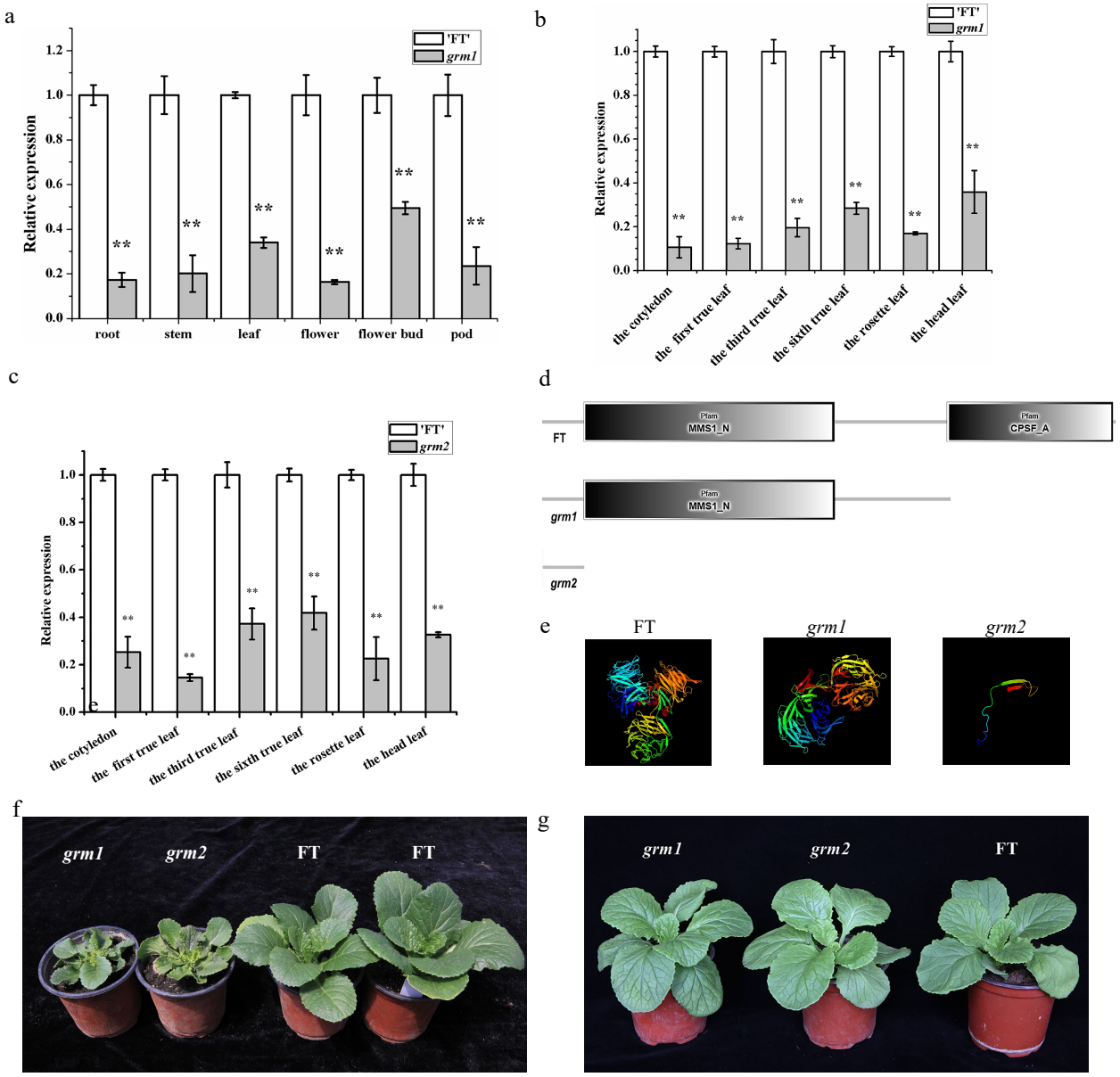

Fig. 7 The expression and protein analyses of *BrDDB1A*. (a) The expression pattern of *BrDDB1A* from different organs of 'FT' and *grm1*. (b) The expression pattern of *BrDDB1A* at different developmental periods from 'FT' and *grm1* leaves. (c) The expression pattern of *BrDDB1A* at different developmental periods from 'FT' and *grm2* leaves. Asterisks indicate significant differences among *grm1*, *grm2* and 'FT' (t test, $P < 0.05$). (d) The analyses of conserved domains of BrDDB1A in 'FT', *grm1*, and *grm2*. (e) Protein tertiary structure of BrDDB1A in 'FT', *grm1*, and *grm2*. (f) The wild-type 'FT', *grm1* and *grm2* plants were cultured in the greenhouse with 1.89 mW/cm^2 UV radiation. (g) The wild-type 'FT', *grm1* and *grm2* plants were cultured indoors with 0.01 mW/cm^2 UV radiation.

environments. When the mutant and wild-type plants were grown in the greenhouse, the mutant plants exhibited the growth retardation phenotype (Fig. 7f). By contrast, when the mutant and wild-type plants were grown indoors, the mutant plants showed wild-type traits, and there were no significant differences between wild-type and mutants in terms of phenotypes (Fig. 7g).

DISCUSSION

Screening mutants by EMS mutagenesis has been widely applied to numerous plants including *Arabidopsis*, rice, wheat, and Chinese cabbage[39–42]. EMS mutagenesis is advantageous because of its high mutation efficiency and diversity of single base mutations and because it results in saturation mutagenesis. In this study, two allelic mutants (*grm1* and *grm2*) were identified from the EMS-mutagenized populations of Chinese cabbage 'FT', whose growth retardation were triggered by the outation of *BraA09g024830.3C* (*BrDDB1A*). EMS is an alkylating agent that largely accomplishes the mutagenesis process as follows: first, the oxygen of the guanine (G) is alkylated. Then, G is paired with thymine (T) during DNA replication. Finally, a base substitution occurs (G:C to A:T). This single base mutation is the main form of EMS mutagenesis. Herein, the *grm1* mutant was obtained by EMS treatment of isolated microspores and its mutated phenotype was caused by the termination of amino acid coding resulted from the deletion of a base (A) in the 17th

exon of *BrDDB1A*. However, the base deletion/insertion mutants did not conform to those of typical EMS mutagenesis. A previous study reported a naturally occurring mutant during microspore culture; Chen et al.[43] obtained a natural stigma exsertion mutant in the isolated microspore culture of ornamental kale. Therefore, we speculated that the *grm1* mutant might be a natural mutant produced during the isolated microspore culture process. In the *grm2* mutant, we found that a base substitution (G-A) occurred in the last base of the first intron, which conformed to typical EMS mutagenesis and resulted in an intron retention event. We speculated that this might have been due to the mutation of the acceptor site of the 3'-end in the alternative splicing event from AG to AA, which destroyed the GT-AG rule of the splicing site.

Allelism test can be used to verify whether the mutations are allelic, that is, the causal gene is the same while the mutated sites occurring in the causal gene might be distinct. In our study, the *grm1* and *grm2* were obtained from EMS-mutagenized populations of wild-type 'FT' isolated-cultured microspores and seeds, respectively. Considering that their growth retardation phenotypes are highly similar to each other, and they possess similar genetic characteristics, we carried out the allelism test between the mutants. The method of the allelism test is crossing two mutants to construct an F_1 generation and observing the phenotype of the F_1 generation. If the phenotype of the F_1 generation is a mutant phenotype, the mutant genes of the two mutants are allelic; if the F_1 generation recovers to a wild-type phenotype, the two mutant genes are complementary and belong to non-allelic genes. Multani et al.[44] obtained a *brachytic2* mutant (*br2*) in maize. The cloned *br2* gene was found to encode a protein that is probably involved in auxin polar transport. Pilu et al.[45] isolated a new *brachytic2* mutant (*br2-23*). The two mutants, *br2* and *br2-23*, were crossed in the allelism test and the F_1 generation phenotype was that of the mutant phenotype; these results indicated that the two mutations of *br2* and *br2-23* are allelic. Our allelism test of the *grm* mutants (*grm1* and *grm2*) showed that their mutations belonged to allelic mutation. Compared with WT, they displayed consistent mutant phenotypes of stunted growth. The causal gene *BrDDB1A* was identified in *grm1* through BSR-Seq combined with whole-genome re-sequencing, and verified by the allele mutations existed in *grm1* and *grm2*. Thus, we suggested that the mutation of *BrDDB1A* triggered the growth retardation in *grm1* and *grm2* mutants of Chinese cabbage.

A previous study showed that DDB1A is involved in the initial damage recognition stage of the NER pathway in response to UV radiation[17,46]. UV stress is considered an important factor affecting the plant growth rate, because the intensity of UV radiation reaching the earth's surface is constantly increasing[47]. UV radiation induces the formation of lesions that can obstruct replication and transcriptional processes and might alter chromatin structure[6,8]. For example, UV radiation can cause a series of morphological changes in rice, such as plant height decreases, leaf thickening, cotyledon curling, stem elongation, leaf expansion, and root ratio (UV radiation plant/normal plant) decreases[48,49]. Increased UV radiation inhibits cotton growth and results in dwarfism[50]. DDB1A recognizes DNA damage and initiates the NER processes[6]. DDB1A might also function to alter chromatin structure and recruit the NER-factor to DNA damage sites[51]. In *Arabidopsis*, the overexpression of DDB1A increases UV-resistance, and the loss of functional mutant in DDB1A results in UV sensitivity[11]. Likewise, the phenotype of the *grm1* and *grm2* mutants was consistent with the morphological changes caused by UV radiation in rice[49]. In our study, we observed that the expression levels of *BrDDB1A* in *grm1* and *grm2* mutants were significantly lower than that in wild-type plants and there was no difference in the promoter sequence between WT and the two allelic mutants. Previous studies in *Arabidopsis* (*DDB1A*), rice (*OsUV-DDB1*) and *Aspergillus nidulans* (*DdbA*) have shown that the mRNA levels of these homologic genes all increased after UV exposure, of which the transcript levels might correlate with the UV-induced DNA repair rate[11,21,52]. Therefore, it was conjectured that the lower mRNA level in *grm* mutants was affected by the failure of dysfunctional BrDDB1A to respond to UV radiation, while the normal BrDDB1A in WT could trigger the function in UV-induced DNA repair, in turn resulting in the higher mRNA level. We also found an interesting phenomenon that when mutant plants were grown indoors under low UV radiation conditions, the mutants exhibited normal growth resembling the wild-type. Therefore, we speculated that the phenotype of *grm1* and *grm2* might be caused by UV radiation damage. Moreover, mutations could have led to changes in the structure of BrDDB1A, making it unable to accurately identify the UV radiation damage site; thus, the NER repair pathway would not be correctly initiated, ultimately resulting in the growth retardation phenotype in Chinese cabbage. This hypothesis requires further investigation.

In summary, we identified *BrDDB1A* as the target gene for the growth retardation in *grm1* and *grm2* mutants. BrDDB1A might be associated with maintaining normal plant growth under UV-stress in Chinese cabbage. This is the first report indicating that *BrDDB1A* functions in maintaining regular plant growth of Chinese cabbage. Our study provides insight for further investigation of the regulatory mechanism of *BrDDB1A* with respect to the growth and development of Chinese cabbage.

ACKNOWLEDGMENTS

The research was funded by the National Natural Science Foundation of China (Grant No. 31730082). We would like to thank Editage (www.editage.cn) for English language editing.

Conflict of interest

The authors declare that they have no conflict of interest.

Supplementary Information accompanies this paper at (https://www.maxapress.com/article/doi/10.48130/VR-2022-0017)

Dates

Received 7 September 2022; Accepted 24 October 2022; Published online 29 November 2022

REFERENCES

1. de Wit M, Galvão VC, Fankhauser C. 2016. Light-mediated hormonal regulation of plant growth and development. *Annual Review of Plant Biology* 67:513–37
2. Yadav A, Singh D, Lingwan M, Yadukrishnan P, Masakapalli SK, et al. 2020. Light signaling and UV-B-mediated plant growth regulation. *Journal of Integrative Plant Biology* 62:1270–92

3. Caldwell MM, Ballaré CL, Bornman JF, Flint SD, Björn LO, et al. 2003. Terrestrial ecosystems, increased solar ultraviolet radiation and interactions with other climatic change factors. *Photochemical & Photobiological Sciences* 2:29–38
4. Manova V, Gruszka D. 2015. DNA damage and repair in plants - from models to crops. *Frontiers in Plant Science* 6:885
5. Kim JH. 2019. Chromatin remodeling and epigenetic regulation in plant DNA damage repair. *International Journal of Molecular Sciences* 20:4093
6. Biedermann S, Hellmann H. 2010. The DDB1a interacting proteins ATCSA-1 and DDB2 are critical factors for UV-B tolerance and genomic integrity in *Arabidopsis thaliana*. *The Plant Journa* 62:404–15
7. Donà M, Mittelsten Scheid O. 2015. DNA damage repair in the context of plant chromatin. *Plant Physiology* 168:1206–18
8. Ly V, Hatherell A, Kim E, Chan A, Belmonte MF, et al. 2013. Interactions between Arabidopsis DNA repair genes *UVH6*, *DDB1A*, and *DDB2* during abiotic stress tolerance and floral development. *Plant Science* 213:88–97
9. Kunz BA, Cahill DM, Mohr PG, Osmond MJ, Vonarx EJ. 2006. Plant responses to UV radiation and links to pathogen resistance. *International Review of Cytology* 255:1–40
10. Roldán-Arjona T, Ariza RR. 2009. Repair and tolerance of oxidative DNA damage in plants. *Mutation Research/Reviews in Mutation Research* 681:169–79
11. Al Khateeb WM, Schroeder DF. 2009. Overexpression of Arabidopsis damaged DNA binding protein 1A (DDB1A) enhances UV tolerance. *Plant Molecular Biology* 70:371–83
12. Al Khateeb WM, Schroeder DF. 2007. *DDB2*, *DDB1A* and *DET1* exhibit complex interactions during Arabidopsis development. *Genetics* 176:231–42
13. Bernhardt A, Mooney S, Hellmann H. 2010. Arabidopsis DDB1a and DDB1b are critical for embryo development. *Planta* 232:555–66
14. Farmer LM, Book AJ, Lee KH, Lin YL, Fu H, Vierstra RD. 2010. The RAD23 family provides an essential connection between the 26S proteasome and ubiquitylated proteins in *Arabidopsis*. *The Plant Cell* 22:124–42
15. Ganpudi AL, Schroeder DF. 2013. Genetic interactions of *Arabidopsis thaliana damaged DNA binding protein 1B* (*DDB1B*) with *DDB1A*, *DET1*, and COP1. *G3 Genes|Genomes|Genetics* 3:493–503
16. Feldberg RS. 1980. On the substrate specificity of a damage-specific DNA binding protein from human cells. *Nucleic Acids Research* 8:1133–43
17. Chu G, Chang E. 1988. Xeroderma pigmentosum group E cells lack a nuclear factor that binds to damaged DNA. *Science* 242:564–67
18. Shuck SC, Short EA, Turchi JJ. 2008. Eukaryotic nucleotide excision repair: from understanding mechanisms to influencing biology. *Cell Research* 18:64–72
19. Levin I, Frankel P, Gilboa N, Tanny S, Lalazar A. 2003. The tomato *dark green* mutation is a novel allele of the tomato homolog of the *DEETIOLATED1* gene. *Theoretical and Applied Genetics* 106:454–60
20. Lieberman M, Segev O, Gilboa N, Lalazar A, Levin I. 2004. The tomato homolog of the gene encoding UV-damaged DNA binding protein 1 (DDB1) underlined as the gene that causes the *high pigment-1* mutant phenotype. *Theoretical and Applied Genetics* 108:1574–81
21. Ishibashi T, Kimura S, Yamamoto T, Furukawa T, Takata K, et al. 2003. Rice UV-damaged DNA binding protein homologues are most abundant in proliferating tissues. *Gene* 308:79–87
22. Oravecz A, Baumann A, Máté Z, Brzezinska A, Molinier J, et al. 2006. CONSTITUTIVELY PHOTOMORPHOGENIC1 is required for the UV-B response in Arabidopsis. *The Plant Cell* 18:1975–90
23. Hayes S, Sharma A, Fraser DP, Trevisan M, Cragg-Barber CK, et al. 2017. UV-B Perceived by the UVR8 Photoreceptor Inhibits Plant Thermomorphogenesis. *Current Biology* 27:120–27
24. Mao X, Kim JI, Wheeler MT, Heintzelman AK, Weake VM, Chapple C. 2019. Mutation of Mediator subunit *CDK8* counteracts the stunted growth and salicylic acid hyperaccumulation phenotypes of an Arabidopsis *MED5* mutant. *New Phytologist* 223:233–45
25. Huang X, Ouyang X, Yang P, Lau OS, Li G, et al. 2012. *Arabidopsis* FHY3 and HY5 positively mediate induction of *COP1* transcription in response to photomorphogenic UV-B light. *The Plant Cell* 24:4590–606
26. Huang S, Liu Z, Yao R, Li D, Feng H. 2015. Comparative transcriptome analysis of the petal degeneration mutant pdm in Chinese cabbage (*Brassica campestris* ssp. *pekinensis*) using RNA-Seq. *Molecular Genetics and Genomics* 290:1833–47
27. Zhang M, Huang S, Gao Y, Fu W, Qu G, et al. 2020. Fine mapping of a leaf flattening gene Bralcm through BSR-Seq in Chinese cabbage (*Brassica rapa* L. ssp. *pekinensis*). *Scientific Reports* 10:13924
28. Lin S, Dong H, Zhang F, Qiu L, Wang F, et al. 2014. *BcMF8*, a putative arabinogalactan protein-encoding gene, contributes to pollen wall development, aperture formation and pollen tube growth in *Brassica campestris*. *Annals of Botany* 113:777–88
29. Kim D, Langmead B, Salzberg SL. 2015. HISAT: a fast spliced aligner with low memory requirements. *Nature Methods* 12:357–60
30. Zhao C, Zhao G, Geng Z, Wang Z, Wang K, et al. 2018. Physical mapping and candidate gene prediction of fertility restorer gene of cytoplasmic male sterility in cotton. *BMC Genomics* 19:6
31. Su A, Song W, Xing J, Zhao Y, Zhang R, et al. 2016. Identification of Genes Potentially Associated with the Fertility Instability of S-Type Cytoplasmic Male Sterility in Maize via Bulked Segregant RNA-Seq. *PLoS One* 11:e0163489
32. Murray MG, Thompson WF. 1980. Rapid isolation of high molecular weight plant DNA. *Nucleic Acids Research* 8:4321–26
33. Schubert M, Lindgreen S, Orlando L. 2016. AdapterRemoval v2: rapid adapter trimming, identification, and read merging. BMC Res Notes 9:88 Accordingly
34. Li H, Durbin R. 2009. Fast and accurate short read alignment with Burrows-Wheeler transform. *Bioinformatics* 25:1754–60
35. Zhu P, He L, Li Y, Huang W, Xi F, et al. 2014. OTG-snpcaller: an optimized pipeline based on TMAP and GATK for SNP calling from ion torrent data. *PLoS One* 9:e97507
36. Wang K, Li M, Hakonarson H. 2010. ANNOVAR: functional annotation of genetic variants from high-throughput sequencing data. *Nucleic Acids Research* 38:e164
37. Rao X, Huang X, Zhou Z, Lin X. 2013. An improvement of the $2^{-\Delta\Delta CT}$ method for quantitative real-time polymerase chain reaction data analysis. *Biostatistics, Bioinformatics and Biomathematics* 3:71–85
38. Guo Y, Yang Y, Huang Y, Shen HB. 2020. Discovering nuclear targeting signal sequence through protein language learning and multivariate analysis. *Analytical Biochemistry* 591:113565
39. Wang Q, Sang X, Ling Y, Zhao F, Yang Z, et al. 2009. Genetic analysis and molecular mapping of a novel gene for zebra mutation in rice (*Oryza sativa* L.). *Journal of Genetics and Genomics* 36:679–84
40. Jin XJ, Sun DF, Li HY, Yang Y, Sun GL. 2013. Characterization and molecular mapping of a dwarf mutant in wheat. *Genetics and Molecular Research* 12:3555–65
41. Derkx AP, Orford S, Griffiths S, Foulkes MJ, Hawkesford MJ. 2012. Identification of differentially senescing mutants of wheat and impacts on yield, biomass and nitrogen partitioning. *Journal of Integrative Plant Biology* 54:555–66
42. Zhang X, Ma W, Liu M, Li X, Li J, et al. 2022. OCTOPUS regulates BIN2 to control leaf curvature in Chinese cabbage. *Proc Natl Acad Sci U S A* 119:e2208978119
43. Chen W, Liu Z, Ren J, Huang S, Feng H. 2019. Identification and fine mapping of a stigma exsertion mutant gene (*Bolsem*) in ornamental kale (*Brassica oleracea var. acephala*). *Molecular Breeding* 39:164
44. Multani DS, Briggs SP, Chamberlin MA, Blakeslee JJ, Murphy AS, et al. 2003. Loss of an MDR transporter in compact stalks of maize br2 and sorghum dw3 mutants. *Science* 302:81–84
45. Pilu R, Cassani E, Villa D, Curiale S, Panzeri D, et al. 2007. Isolation and characterization of a new mutant allele of *brachytic 2* maize gene. *Molecular Breeding* 20:83–91

46. Li J, Wang QE, Zhu Q, El-Mahdy MA, Wani G, et al. 2006. DNA damage binding protein component DDB1 participates in nucleotide excision repair through DDB2 DNA-binding and cullin 4A ubiquitin ligase activity. *Cancer Research* 66:8590–97
47. Lee K, Kang H. 2016. Emerging roles of RNA-Binding proteins in plant growth, development, and stress responses. *Molecules and Cells* 39:179–85
48. Frohnmeyer H, Staiger D. 2003. Ultraviolet-B radiation-mediated responses in plants. Balancing damage and protection. *Plant Physiology* 133:1420–28
49. Caldwell MM, Bornman JF, Ballaré CL, Flint SD, Kulandaivelu G. 2007. Terrestrial ecosystems, increased solar ultraviolet radiation, and interactions with other climate change factors. *Photochemical & Photobiological Sciences* 6:252–66
50. Ambler JE, Krizek DT, Semeniuk P. 1975. Influence of UV-B radiation on early seedling growth and translocation of ^{65}Zn from cotyledons in cotton. *Physiologia Plantarum* 34:177–81
51. Gillet LC, Schärer OD. 2006. Molecular mechanisms of mammalian global genome nucleotide excision repair. *Chemical Reviews* 106:253–76
52. Lima JF, Malavazi I, da Silva Ferreira ME, Savoldi M, Mota AO Jr, et al. 2008. Functional characterization of the putative *Aspergillus nidulans* DNA damage binding protein homologue DdbA. *Molecular Genetics and Genomics* 279:239–53